Journal of
Oral Pathology & Medicine

doi: 10.1111/jop.12251

J Oral Pathol Med

wileyonlinelibrary.com/journal/jop

The low-affinity nerve growth factor receptor p75NTR identifies a transient stem cell-like state in oral squamous cell carcinoma cells

Tarig A. Osman[1,2], Himalaya Parajuli[1,2], Dipak Sapkota[1], Israa A. H. Ahmed[1,2], Anne Ch. Johannessen[1,3], Daniela Elena Costea[1,3,4]

[1]*Gade Laboratory for Pathology, Department of Clinical Medicine, Faculty of Medicine and Dentistry, University of Bergen, Bergen, Norway;* [2]*Department of Global Public Health and Primary Care, Center for International Health, Faculty of Medicine and Dentistry, University of Bergen, Bergen, Norway;* [3]*Department of Pathology, Haukeland University Hospital, Bergen, Norway;* [4]*Department of Biomedicine, Faculty of Medicine and Dentistry, University of Bergen, Bergen, Norway*

BACKGROUND: Although several markers have been used for enrichment of cells with stem cell-like properties in oral squamous cell carcinoma (OSCC), isolation of a pure subpopulation is still a challenging task. Normal oral and esophageal keratinocyte stem cells have been previously isolated using the low-affinity nerve growth factor receptor p75NTR.

OBJECTIVE: To investigate the potential of p75NTR as a marker for identification and isolation of oral cancer cells with stem cell-like properties.

METHODS: Subpopulations of cells with high or low expression of p75NTR were sorted from OSCC-derived cells and compared for sphere/colony formation, *in vivo* tumor formation ability, expression of stem cell-related molecules, cell cycle distribution and drug resistance.

RESULTS: p75NTR^{High} cells exhibited statistically significant higher stem cell properties than p75NTR^{Low} cells in all assays performed. Nevertheless, p75NTR^{Low} subpopulation did also exhibit some stem cell features, but to a lesser extent. Propagation of p75NTR^{Low} cells for several passages in culture showed that the expression of p75NTR could rise spontaneously. This finding was also supported by the similar expression of p75NTR by the xenografts generated by both subpopulations in NOD \SCID IL2Rg^{null}mice.

CONCLUSION: p75NTR can be used for isolating a subpopulation enriched for cells with stem cell-like properties in OSCC. *De novo* generation of p75NTR^{High} cells from p75NTR^{Low} cells suggests either that there is another subpopulation with stem cell features within the p75NTR^{Low} cells, or that the p75NTR^{Low} cells can dedifferentiate due to a contextually regulated equilibrium between stem cell-like cells and transit-amplifying neoplastic progenitors.

J Oral Pathol Med (2014)

Keywords: cancer stem cell; oral squamous cell carcinoma; p75NTR; plasticity; stochastic stem cell; tumor heterogeneity

Correspondence: Tarig A. Osman, Gade Laboratory for Pathology, University of Bergen, Haukeland University Hospital, Central block, 2nd floor, N-5021 Bergen-Norway. Tel: +47 40 30 4962, Fax: +47 55 97 3158, E-mail: tos094@gades.uib.no
Accepted for publication July 19, 2014

Introduction

The notion that tumor growth is driven by a subpopulation with stem cell properties, referred to as cancer stem-like cells (CSCs), or tumor-initiating cells (TIC), has attracted much attention during the last decade (1). Research in acute myeloid leukemia (AML) provided the first persuasive proof of the CSC theory (2, 3). Those pivotal findings have led to the investigation of the existence of CSCs in many solid tumors, and their presence has been shown in several solid malignancies, such as breast (4), colon (5), brain (6), prostate (7), lung (8), liver (9), and melanoma (10). In some human cancers, a role for CSCs in tumor recurrence (11), chemotherapy resistance (12), and metastasis (13) has been suggested. Therefore, it has been theorized that identification of distinctive phenotypical characteristics of CSCs would provide a promising target for a better, more targeted, and efficient form of cancer treatment. Analogical to normal adult stem cells, CSCs are defined as the cells with (i) self-renewal ability/tumor initiation ability and (ii) the ability to generate all more differentiated phenotypes forming the bulk cells of a tumor (1). The experimental functional CSC assays are thus aimed to investigate those distinctive features. Xenotransplantation into animal models, also known as *in vivo* tumor formation assay, is the most

accepted CSC/TIC assay, despite of its inadequacies, and it is considered the benchmark for other assays (1). Sphere formation assay is based on the ability of stem cells to self-renew and grow independent of anchorage, and it is considered the *in vitro* surrogate for the *in vivo* tumor formation assay (14).

Although the CSC model has been proven in some human cancers, the available evidence in others cannot refute that the difference in the tumorigenicity of cancer cells and phenotypic heterogeneity can also arise as a result of the genetic instability, and expansion of mutated clones (15, 16). Moreover, it has been recently shown in metastatic colon cancer that the two models can coexist, by observing that chromosomal instability takes place preferentially in cells exhibiting CSC behavior (17). The plasticity of tumor cells might also play a role, and a switching of CSC between different phenotypes was reported in oral squamous cell carcinoma (OSCC) (18) and breast cancer (19).

In OSCC, the most common type of head and neck cancers, several subpopulations have been reported to be enriched for CSCs. Among these, $CD44^{High}$ (20), $ALDH1^{High}$ (21), and the side population (22) have been suggested. However, a pure CSC subpopulation is yet to be identified, and recent evidence suggests that the cancer stemness is a rather dynamically regulated phenotype than a distinct entity. The low-affinity nerve growth factor receptor p75NTR was described as a putative marker of normal oral (23) and esophageal (24) keratinocyte stem cells. Although structurally belonging to the tumor necrosis factor receptor superfamily (25), many of the biological functions of p75NTR differ from other members of this family, and a role in promoting cell survival has been suggested in normal human oral mucosa (NHOM) (23) and nerves (26). Furthermore, possible role of this molecule in carcinogenesis was suggested in laryngeal, prostate, and breast cancers (27–29). It has also been suggested as a marker of CSCs in malignant melanoma (30), esophageal carcinoma (31), and it was found to be a determinant of poor prognosis in OSCC (32, 33). Nevertheless, recent data from 3D stepwise models of OSCC indicated a loss of CD44 and p75NTR hierarchical coordination with OSCC progression (34), bringing more controversy into the issue of phonotypical markers, such as p75NTR or CD44, as good markers for stem cell identification and isolation.

In AML, markers of normal stem cells of the tissue of origin have been successfully used to isolate CSCs (2); therefore, we hypothesized that p75NTR, as a marker of normal oral keratinocyte stem cells, comprises a putative CSC marker in OSCC.

Materials and methods

Cell culture

Oral squamous cell carcinoma-derived cells of the cell lines, known as CalH3 (p53 wild) and 5PT (p53 mutated) (35), were grown in Dulbecco's modified Eagle's medium (*DMEM)* supplemented with 25% *nutrient mixture F-12 Ham*, 50 μg/ml L ascorbic acid, 0.4 μg/ml hydrocortisone, 10 ng/ml epidermal growth factor (all from Sigma-Aldrich, Saint Louis, MO, USA), 10% fetal bovine serum (FBS), and 5 μg/ml insulin (both from Life Technologies, Carlsbad, CA, USA), also known as FAD medium (36), under standard culture conditions. Cells were used at 16–24 passages.

Fluorescent-activated cell sorting (FACS)

Cells were detached at 70–80% confluency using 1× *trypsin-EDTA* (Sigma-Aldrich), counted and resuspended in phosphate-buffered saline (PBS) containing FBS and *HEPES* (Life technologies) as 1% each. Afterward, cells were incubated with mouse monoclonal anti-p75NTR antibody (clone ME20.4, 1:250; Sigma) for 10 min on ice. *Negative control mouse IgG1* (1:250; Dako, Golstrup, Denmark) was used as an isotype control. After a washing step, cells were incubated with Alexa Fluor® 488 $F(ab^1)2$ fragment of goat anti-mouse H+L (1:250; Life technologies) for another 10 min on ice and protected from light. All FACS procedures were performed with *BD FACSAria™IIu* (BD Biosciences, Franklin Lakes, NJ, USA), using 525/50 BP filter. Cells with considerably small size or smooth surface (apoptotic), as well as doublets, were gated out according to forward- and side-scattered light, and further analysis was performed only on the main population of cells. The highest and lowest 5% of the cells were sorted and collected in FAD medium. All sorts were followed by post-sort FACS checking. Independent sorts were carried out at different passages.

Colony formation assay

Cells sorted according to expression of p75NTR were seeded in 6-well plates as 500 cells in 3 ml of FAD medium/well and allowed to grow under standard culture conditions for 7–15 days. After examining microscopically, wells were washed with PBS, and 2 ml of cold 4% paraformaldehyde (Sigma-Aldrich) was added to fix the colonies. The wells were washed again after 10 min and stained with 0.5% crystal violet (Sigma). The minimum number of cells in a colony was set to 50 cells, and calibration to the minimum size of a colony was made before counting the colonies macroscopically. Independent experiments were performed for three different passages.

Sphere formation assay

To prepare non-adherent culture plates, 1% solution of poly 2-hydroxyethyl methacrylate (*pHEMA*; Sigma) in ethanol was used to coat 96-well plates. Five hundred $p75NTR^{High}$ or $p75NTR^{Low}$ CalH3 cells were resuspended in a mixture of 475 ml of FAD medium and 25 μl of *Matrigel* (BD Bioscience) and loaded into each well. Cells were allowed to grow for 2 weeks under standard culture conditions, and the number of spheres was counted under an inverted microscope. Independent experiments were performed at three different passages.

Cell cycle analysis

Unsorted, $p75NTR^{High}$ and $p75NTR^{Low}$ CalH3 cells were fixed using chilled 70% ethanol for 1 h on ice, washed in chilled PBS, and centrifuged at 300 g for 5 min at 4°C degrees. Cells were incubated with propidium iodide (PI) solution for half an hour at 37°C in the dark. For every one million cells, PI solution consisted of 50 μl of PI (1000 μg/ml; Life technologies), 125 μl of RNAse (1 mg/ml; Sigma), 380 μl of Na citrate (100 nM), and 445 μl of 1× PBS. Cells

were then washed and centrifuged again in PBS and analyzed in *Accuri6* cytometer (BD Biosciences). For each sample, at least 30 000 events were recorded and analyzed in *Flowjo* version 10 (Tree star Inc., Ashland, OR, USA) using Dean–Jett–Fox model. Three independent experiments performed at different passages were performed.

Drug resistance assay

Sorted cells were seeded in 96-well plate at density of 5000 cells/well and allowed to grow in FAD medium. After 48 h, the medium was replaced by 100-μl fresh FAD medium containing 5-fluorouracil (Sigma) at concentration of 0, 2, 4, 8, 16, or 32 μg/μl in quadruplicates and kept under standard culture conditions for another 48 h. Afterward, 10 μl of *WST-1* (Roche Applied Sciences, Penzberg, Germany) was added to each well, and the light absorbance was read 2–3 h later at 440 nM wavelength in *FLUOstar Omega plate* reader (BMG LABTECH, Ortenberg, Germany). The difference in the absorbance between the two phenotypes at each of the drug concentration used was investigated as a paired sample. Four independent experiments performed at different passages were carried out.

In vivo tumor formation assay

The animal experiments were approved by the Norwegian Animal Research Authority. The animals used were 20 NOD\SCID IL2Rg^{null} mice (n = 10 in each group) (Jackson Laboratories, Bar Harbour, ME, USA). Five thousand p75NTR^{High} or p75NTR^{Low} CalH3 cells were suspended in 25 μl of *Matrigel* and injected into the tongues of the mice under anesthesia with isoflurane (Isoba VetTM) (Schering Plough, Kenilworth, NJ, USA) (3% induction and 1% maintenance). The mice were examined for tumor formation every week, starting 2 weeks from the day of injection and measured bidirectionally using a caliber, under gas anesthesia. Tumor size was calculated using the following formula: volume = $(\text{width})^2$ * length/2. Animals were sacrificed after 53 days, and tongues were collected, in addition to the locoregional lymph nodes when visible, fixed in formalin and embedded in paraffin. Tumor formation was confirmed using H&E stained sections. Means of the tumor sizes as recorded every week were compared between the two animal groups in a pairwise manner.

Immunohistochemistry (IHC)

Formalin-fixed paraffin-embedded samples were cut into 3- to 4-μm sections as duplicates on each slide. Sections were then deparaffinized and rehydrated by immersion in xylene and diminishing concentrations of alcohol. Retrieval of the epitope was performed by heating the sections in a microwave oven in a pH 6.0 *target retrieval buffer* (Dako). For p75NTR staining, sections were incubated with 1× trypsin for 10 min at 42°C. Endogenous enzyme activity and unspecific binding were blocked using *peroxidase block* and 10% normal goat serum, respectively (both from Dako). Sections were then incubated over night at 4°C with one of the following monoclonal mouse anti-human primary antibodies: anti-Ki-67 (1:1500; Dako), anti-p75NTR (1:1000; Sigma), and *Novcastra™* anti-involucrin (1:1000; Leica Biosystems, Wetzlar, Germany). *Envision+®* *anti-mouse* (Dako) was used to detect the site of reaction according to the manufacturer's instructions. And the reaction was visualized using 3,3′-diaminobenzidine tetrahydrochloride (DAB). Incubation with primary antibody was omitted for negative control sections, and NHOM samples have been used as a positive controls (37). Sections were then counterstained with hematoxylin (Dako), dehydrated, and cover-slipped.

Evaluation of IHC

Sections subjected to IHC were evaluated by the principal investigator (TO) after calibration with another investigator (DS) using a light microscope equipped with ×63 objective (Leica) and Zeiss digital camera operated by Zen 2011 software (Carl Zeiss AG, Jena, Germany). The labels of the slides were covered, and four random fields were evaluated. Frequency of p75NTR-positive cells was evaluated semi-quantitatively and scored into four levels (0: <5%, 1: 5–25%, 2: 26–50%, and 3: >50%). Frequency of Ki-67-positive cells was quantified as percentage of the total number of cells/field, and the mean percentage of each section was calculated. The difference between the means of IHC scores, for both p75NTR and Ki-67, was investigated. For evaluation of involucrin staining, slides were scanned using *Scanscope® XT* (Aperio, Vista, CA, USA) using 20× objective, and *color deconvolution algorithm*, version 9.1, was employed to measure the total staining area and intensity of the staining, using default parameters of the algorithm (37). From the algorithm output, mean staining score (1.0*(%weak) + 2.0*(%medium) + 3.0*(%strong) was compared between samples from the two animal groups. Additionally, difference in the mean of the total optical density was investigated.

Quantitative reverse transcriptase PCR

Total RNA was extracted from both p75NTR^{High} and p75NTR^{Low}CaLH3 cells using *RNeasy fibrous tissue mini kit* protocol (Qiagen, Venlo, Limburg, the Netherlands). Following manufacturer's instructions, 300 ng of total RNA was converted to cDNA using *High-Capacity cDNA Archive Kit system* (Life technologies). All qRT-PCR amplifications were performed on *ABI Prism Sequence Detector 7900 HT* (Life technologies) as described previously (38). qRT-PCR was performed to examine the expression levels of the following genes (*TaqMan assays*): *NGFR* (Hs00609947_m1), *PDPN* (Hs00366766_m1), *CD44* (Hs01075861_m1), *POU5F1* (Hs 00999632_g1), *BMI1* (Hs00180411_m1), *VIM* (HS00185584_m1), *KRT10* (HS00166289_m1), and *IVL* (HS00902520_m1), encoding p75NTR, podoplanin, CD44, Oct4, BMI1, vimentin, cytokeratin 10, respectively. Comparative $2^{-\Delta\Delta}$ Ct method was used to quantify the relative mRNA expression, and *GAPDH* (Hs99999905_m1) was used as endogenous control.

Statistical analysis

Analysis of the qRT-PCR data was performed in *GraphPad Prism 6* (GraphPad, La Jolla, CA, USA), while all other statistical procedures were conducted in *Statistical Package for Social Sciences* (SPSS), version 19 (IBM, Armonk, NY, USA). Normality of the distributions of continuous variables was explored using Shapiro–Wilk test. Differences in the means were investigated either with Student's t-test or with Mann–Whitney U-test, as the parametric and the

non-parametric tests of choice, respectively. Pairwise comparison of the tumor growth between the two xenograft groups, or the light absorbance in the drug resistance assay, was investigated by related samples Wilcoxon signed rank test. In all statistical procedures, the level of significance was set to 0.05.

Results

p75NTR^{High} cells showed higher ability than p75NTR^{Low} cells to form colonies and spheres in vitro

The expression of p75NTR was found to have a gradient pattern, and no well-separated positive and negative subpopulations were found by FACS analysis (Fig 1A, B). Therefore, the highest and lowest 5% p75NTR-expressing cells were defined as p75NTR^{High} and p75NTR^{Low} cells (Fig. 1C). The FACS procedure (Fig. 1A–C) yielded constantly highly pure sorted subpopulations of p75NTR^{High} (98.2% ± 0.87 in CaLH3 and 98.6% ± 0.24 for 5PT) and p75NTR^{Low} (98.8% ± 0.84 in CaLH3 and 98.2 ± 0.59 for 5PT) cells, as confirmed by repeating the FACS analysis for part of the sample immediately after the sorting session (Fig. 1D, Figure S1B) and by subsequent qRT-PCR of the sorted cells (Fig. 2A). Both subpopulations of cells sorted for high and low expression of p75NTR were found to be able to form spheres, but the number of spheres formed by p75NTR^{High} cells was found to be significantly higher (P = 0.000 for both cell lines); the number of spheres formed by p75NTR^{High} cells comprised 4.14% ± 1.28 for CaLH3 and 12.8% ± 3.97 for 5PT of the total number of cells seeded, compared to only 1.7% ± 0.58 and 3.8% ± 2.92% for p75NTR^{Low} cells in CaLH3 and 5PT, respectively (Fig. 2C, D). Colony formation assay revealed that significantly higher percentage (44% ± 2.58 for CaLH3 and 16.4 ± 13.03 for 5PT) of p75NTR^{High} cells formed colonies when compared to p75NTR^{Low} cells (25.3% ± 3.4, P-value = 0.000 for CaLH3 and 13.02 ± 2.4, P = 0.038 for 5PT) (Fig. 2E, F).

p75NTR^{High} cells were more tumorigenic than p75NTR^{Low} cells in vivo

The incidence of tumor formation was found to be higher in mice injected with p75NTR^{High} than in mice injected with p75NTR^{Low} CaLH3 cells (90% and 70%, respectively). The most striking difference in the incidence of tumor formation was observed at early stages (70% for p75NTR^{High} compared to 30% for p75NTR^{Low} at the first reading), which indicated a longer lag phase for tumor formation of p75NTR^{Low} cells (Fig. 3A). Although tumor sizes were found to be heterogeneous within each of the two groups, pairwise comparison of the mean tumor size between the two animal groups at each of the time points showed that tumors generated by p75NTR^{High} cells were growing significantly bigger than the tumors generated by p75NTR^{Low} cells (P-value = 0.043, Wilcoxon signed rank test) (Fig. 3B).

p75NTR^{High} cells expressed higher levels of stem cell-related markers than p75NTR^{Low} cells

qRT-PCR revealed that compared to p75NTR^{Low} cells, the p75NTR^{High} CaLH3 cells had significantly higher expression levels of surface markers previously reported as CSC markers, namely CD44 and D2-40. Additionally, expression

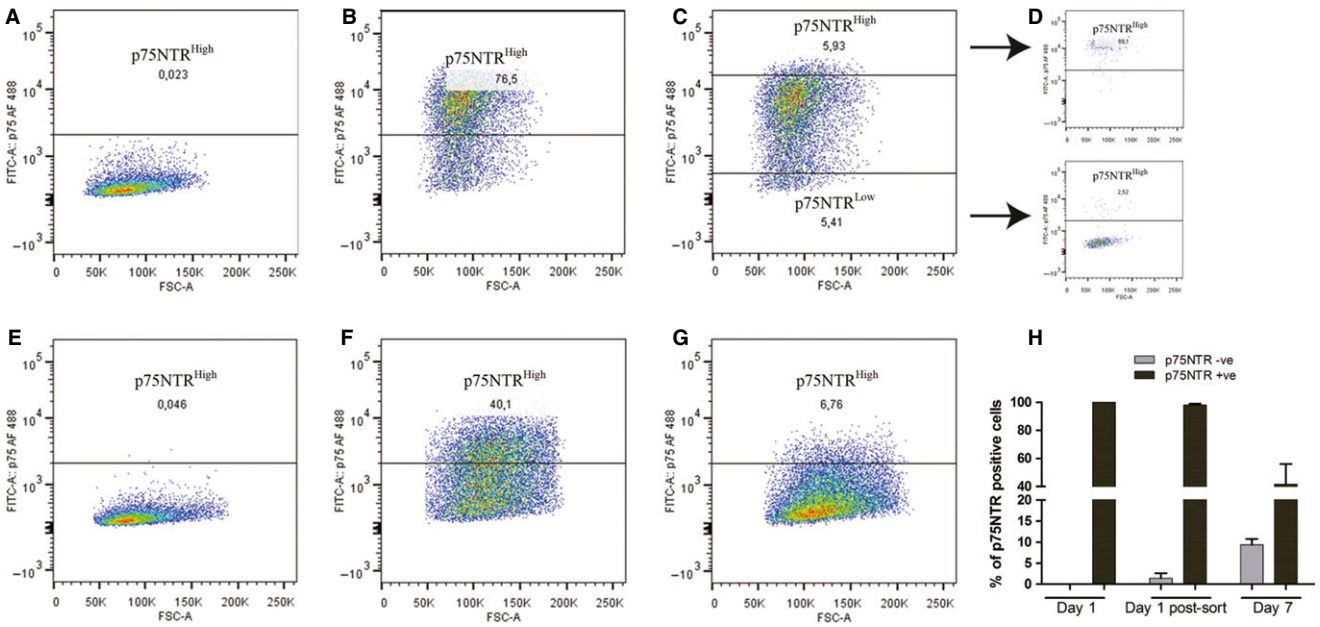

Figure 1 Fluorescent-activated cell sorting (FACS) of oral squamous cell carcinoma (OSCC)-derived cells (CaLH3 cell line) according to p75NTR expression. Cells immunostained with isotype control (A) were used to set the positive signal threshold for cells immunostained with anti-P75NTR antibody (B). The highest and lowest 5% of the cells were sorted accordingly (C), followed by post-sorting check (D). p75NTR^{High} cells immunostained with isotype control after propagation in culture for 7 days (E), and the same gate as in A was found applicable. p75NTR^{High} (F) and p75NTR^{Low} (G) cells immunostained with anti-p75NTR antibody after propagation for 7 days in culture, same gate as in A and E. Bar chart illustrating the change in the percentage of p75NTR +ve and −ve CaLH3 cells from day 1 to day 7 (H). Error bars represent standard deviation.

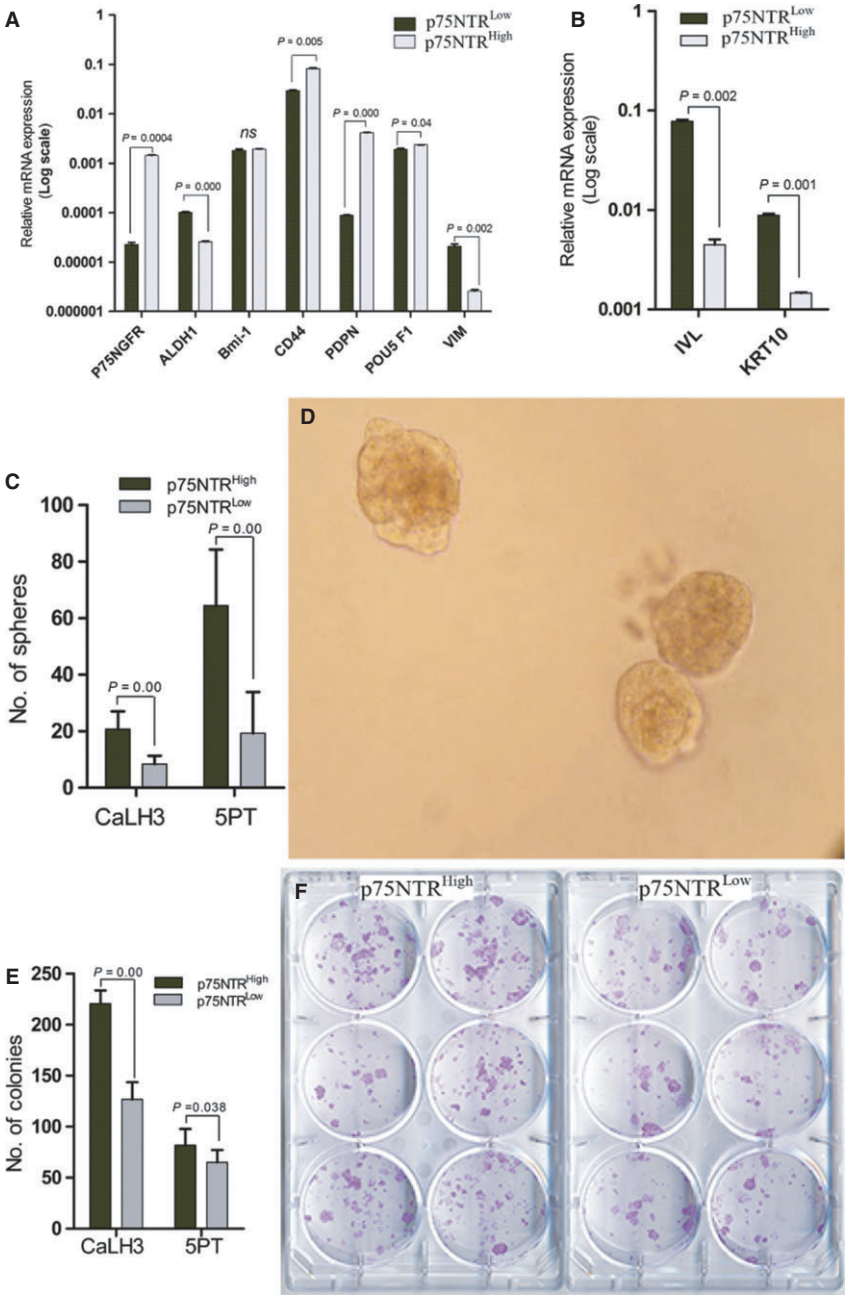

Figure 2 Comparison of the means of the expression levels, in a logarithmic scale, of stem cell- and epithelial-to-mesenchymal transition (EMT)-related markers (A), and differentiation markers (B) in p75NTR^{High} and p75NTR^{Low} CalH3 cells, as yielded by qRT-PCR. Difference in sphere (C, D) and colony (E, F) formation abilities between p75NTR^{High} and p75NTR^{Low} CaLH3 and 5PT cells. Error bars represent standard deviations.

of the more universal/embryonal stem cell marker Oct-4A was found to be significantly higher in p75NTR^{High} CaLH3 cells, while the epithelial-to-mesenchymal transition (EMT) marker vimentin and stem cell and EMT-/CSC-related marker ALDH1 were found expressed at a lower level by p75NTR^{High} CaLH3 cells. Higher expression of the differentiation markers (CK-13 and involucrin) by p75NTR^{Low} CaLH3 cells was also found to be significantly different from that of p75NTR^{High} cells (Fig. 2A,B). p75NTR^{High} 5PT cells showed also lower expression of the differentiation markers (CK10) and EMT marker vimentin, but significantly higher expression of the CSC stem cell marker ALDH1 only (Figure S1A).

Higher percent of p75NTR^{High} cells were at the G2 phase and displayed significantly higher drug resistance than p75NTR^{Low} cells

Higher proportion of p75NTR^{High} CaLH3 cells (32.07% ± 9.2) were found to be at G2 phase compared to p75NTR^{Low} cells (8.91% ± 3.34) and the unsorted cell population (22.15% ± 9.02) (Fig. 4A–C). The drug resistance assay showed that p75NTR^{High} cells were

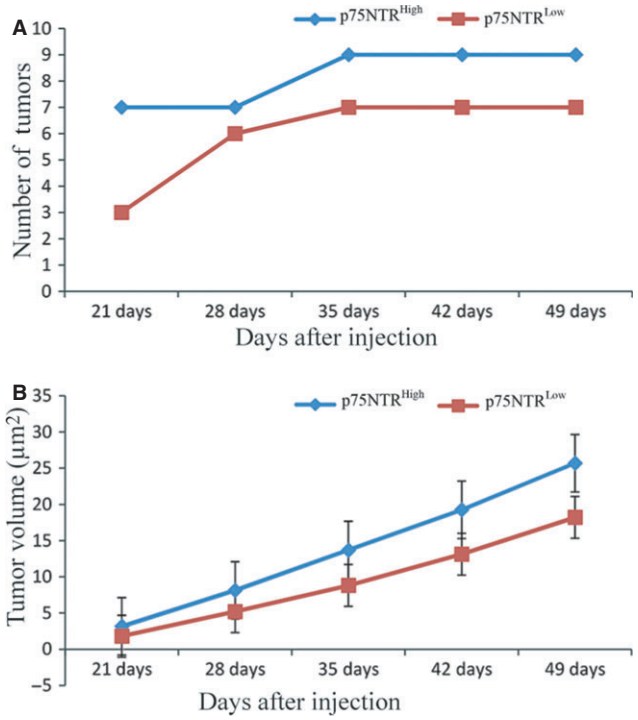

Figure 3 Comparison of the tumor formation incidence and tumor sizes between animals injected with 5000 p75NTR^{High} or p75NTR^{Low} CaLH3 cells at each of the five time points. Error bars represent standard deviations.

more resistant to5-fluorouracil than p75NTR^{Low} cells (Fig. 4D).

Xenografts formed by both p75NTR^{High} and p75NTR^{Low} cells contained a subpopulation of P75NTR+ cells

Tumor xenografts formed by both p75NTR^{High} and p75NTR^{Low} CaLH3 cells showed a typical OSCC tumor morphology, well differentiated, with keratin pearl formation and invasion in the surrounding tongue musculature (Fig. 5A, B). No difference between the xenografts generated by the two different subpopulations of cells was observed for the frequency of p75NTR-, Ki-67-, or involucrin-positive cells (Table 1, Fig. 5C–H). Of interest, a stronger intensity of involucrin staining, evident by higher staining score and total optical density (*P*-value = 0.008, 0.005, respectively), was observed in p75NTR^{High} xenografts (Table 1).

p75NTR^{High} cells could arise de novo *from the p75NTR^{Low} cells*

To investigate the dynamic of p75NTR^{High} and p75NTR^{Low} subpopulations overtime, sorted subpopulations were further propagated *in vitro* for a week, and FACS analysis was performed as done before. The cell population arising from the p75NTR^{High} cells was found to contain only 41.6% ± 14.45 and 88.15% ± 1.7 p75NTR-positive cells in CaLH3 and 5PT, respectively, as compared to the concomitant isotype controls, indicating their ability to regenerate both p75NTR^{Low} and p75NTR^{High} phenotypes

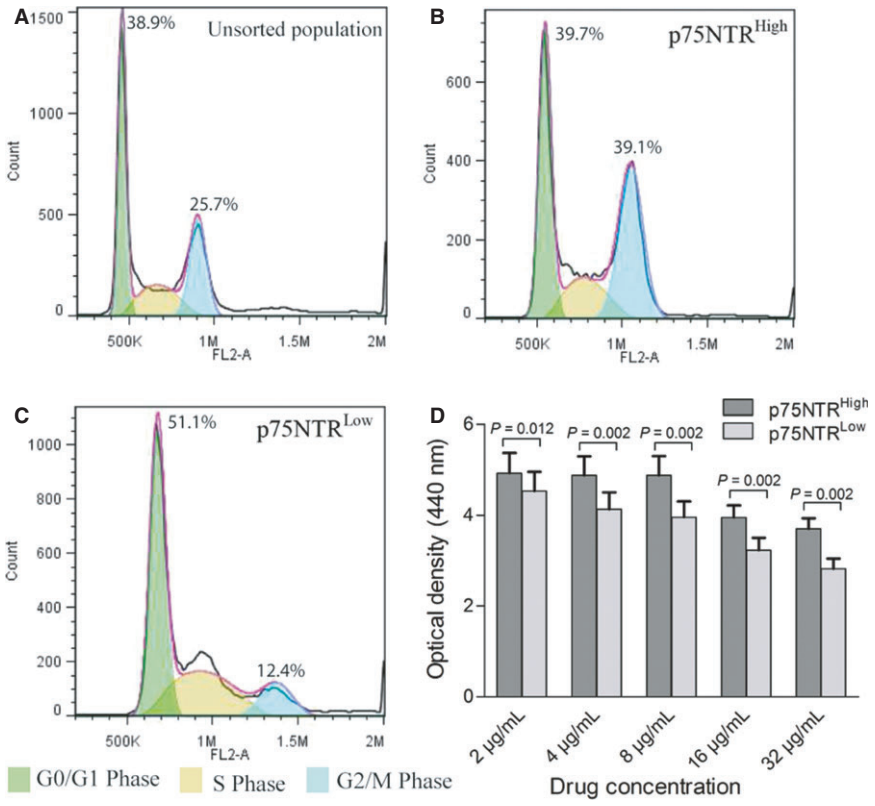

Figure 4 Cell cycle distribution of unsorted oral squamous cell carcinoma (OSCC)-derived cells (CaLH3 cell line) (A), p75NTR^{High} (B), and p75NTR^{Low} (C) cells using Dean–Jett–Fox model. Comparison of the mean light absorbance between p75NTR^{High} and p75NTR^{Low} cells in CaLH3 and 5PT cell lines, after 48-hour exposure to 5-fluorouracil, and 2- to 3-hour incubation with *WST-1*(D). Error bars represent standard error of the mean.

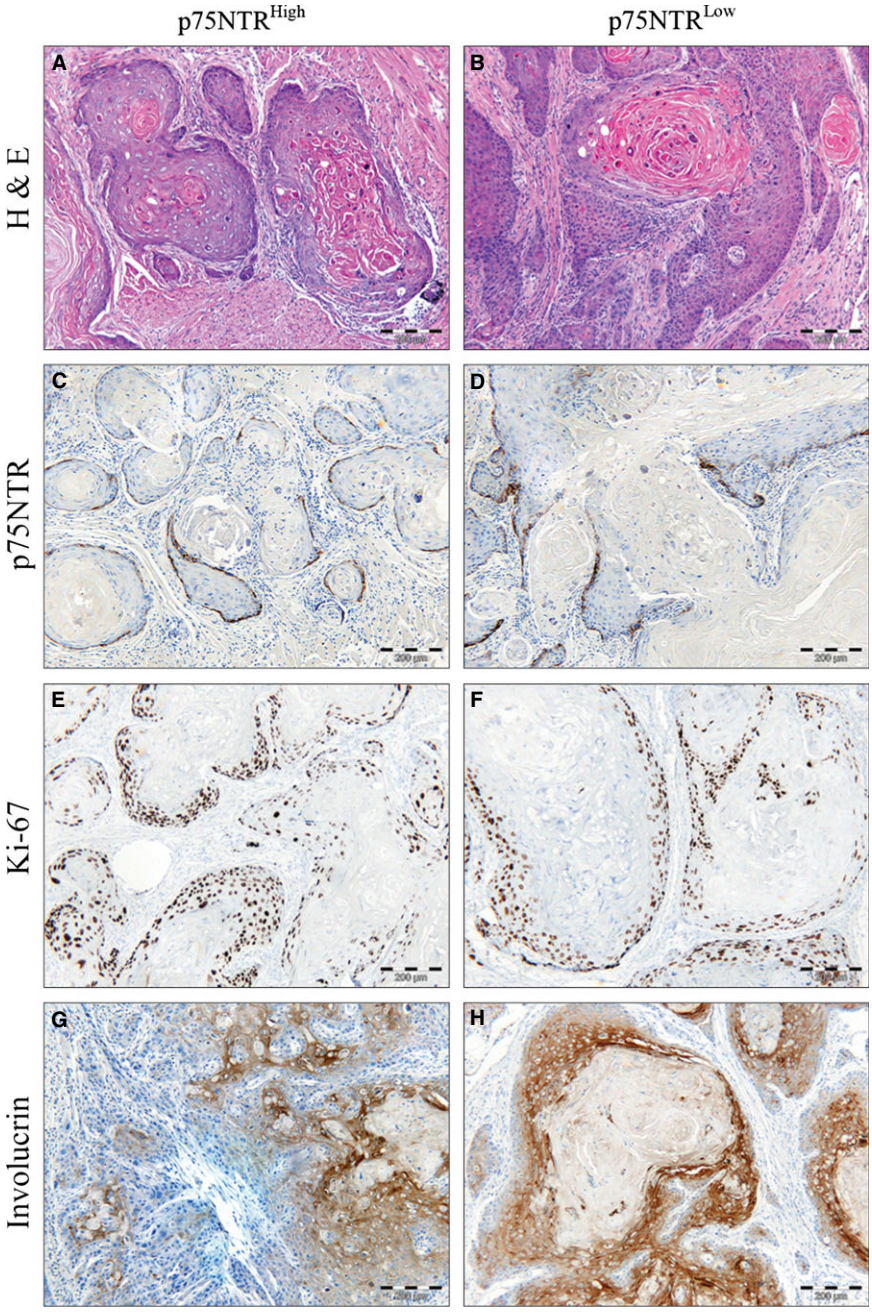

Figure 5 Histological sections of tumor xenografts generated by p75NTR^{High} (left) and p75NTR^{Low} (right) cells. Sections stained with hematoxylin and eosin (A, B), immunostained (brown color) for p75NTR (C, D), Ki-67 (E, F), and Involucrin (G, H). Immunohistochemically stained sections were counterstained with hematoxylin.

of OSCC cells. Interestingly, a subpopulation of p75NTR-positive cells (9.4% ± 1.37 in CaLH3 and 4.1% ± 0.28 in 5PT) was also found in the cells arose from the parallel p75NTR^{Low} cells (Fig. 1E–H, Figure S1B), indicating as well their ability to regenerate both p75NTR^{Low} and p75NTR^{High} phenotypes of OSCC cells.

Discussion

The results of this study showed that the p75NTR^{High} OSCC cells are enriched in cells with stem cell-/tumor-initiating abilities. It is known that monolayer culture conditions alter the normal pattern of differentiation and proliferation of cells and are not as accurate in restoring the original phenotype as the 3D cultures for example (34), but despite of this, cells with clonogenic properties and expression patterns similar to those of TICs *in vivo* were shown to persist in malignant cell lines and show similar cell cycle characteristics and apoptotic resistance with the *in vivo* ones (39). Thus, in addition to *in vitro* assays using OSCC-derived cell lines, we have performed *in vivo* tumorigenic assays as well, injecting cells at a low concentration

Table 1 Comparison of the immunohistochemistry (IHC) scores of p75NTR and Ki-67, and the total optical density and the staining scores of involucrin between xenografts generated by p75NTR^{High} ($N = 9$) and p75NTR^{Low} ($N = 7$) CaLH3 cells

Parameter quantified after IHC	*Xenograft type*	*Mean*	*Median*	*SD*	*P-value*
p75NTR score	P75NTR^{High}	1.167	1.00	0.217	1.000
	P75NTR^{Low}	1.179	1.00	0.238	
Ki-67 score	P75NTR^{High}	52.207	53.605	11.482	0.210
	P75NTR^{Low}	59.603	54.512	11.450	
Involucrin score	P75NTR^{High}	56.712	53.408	8.227	0.008
	P75NTR^{Low}	77.243	72.831	17.302	
Involucrin total optical density	P75NTR^{High}	3.797	3.542	0.699	0.005
	P75NTR^{Low}	6.124	5.609	2.142	

(5000 cells/injection). Compared to p75NTR^{Low} cells, this subpopulation was found to have higher tumor formation incidence, with shorter lag phase and faster growth rate when transplanted at the same low injection number into immune-deficient mice. *In vitro* assays revealed that p75NTR^{High} cell subpopulation had more sphere/colony formation and drug resistance abilities. Cell cycle analysis showed a high percentage of p75NTR^{High} cells at the G2 phase, a phenomena that was previously showed to be a characteristic of normal and malignant epithelial stem cells (40). These results are also in line with the ones of Urdiales et al. (41), which found on rat adrenal gland PC12 cells that p75NTR was expressed mainly in late G1, S, and G2 phases and that signaling in this phases would promote more survival. The p75NTR^{High} cell subpopulation was also more resistant to drug treatments in both OSCC cell lines tested here, corroborating the suggestion of Urdiales et al. that signaling in this cell cycle phase is relevant more for survival then for differentiation. Moreover, expression of several stem cell markers was found to be higher in this subpopulation. This is in line with previous studies from normal tissues, showing that sorting for p75NTR alone is sufficient to enrich for cells with stem cell-like properties both in oral mucosa (23, 42) and esophagus (24), as well as in esophageal cancer (43). Of interest, expression of EMT–CSC marker ALDH1(18) and the EMT-related marker vimentin was lower in the p75NTR^{High}, suggesting that p75NTR selects preferentially the epithelial phenotype of the CSC in oral carcinomas.

Nevertheless, p75NTR^{Low} subpopulation exhibited also, although to a lesser extent, some stem cell abilities. The stem cell behavior found in the p75NTR^{Low} subpopulation could be thought of as a technical failure of a pure sorting, as a result of a dedifferentiation of the p75NTR^{Low} cells, or as a manifestation of another subpopulation with stem cell features within the p75NTR^{Low} cells. Our post-sorting, systematically performed for all of our experiments, indicated the first alternative as less likely to be the cause of the stem cell behavior of the p75NTR^{Low} subpopulation. We are therefore more inclined to consider the other alternatives more likely to be the cause of our observations. Using the same antibody for both FACS analysis and IHC, we found that p75NTR-positive (+ve) cells could arise from the more differentiated p75NTR negative (−ve) cells, both *in vivo* and *in vitro*. *De novo* generation of p75NTR^{High} cells from p75NTR^{Low} cells might be the result of a contextually regulated equilibrium between stem cell-like cells and transit-amplifying neoplastic progenitors and thus could be interpreted as a consequence of a dedifferentiation occurring in the progenitor cells. It has been previously argued that the hierarchy of cancer cell population suggested by the CSC model must coexist with other phenomena that can lead to tumor heterogeneity, including clonal expansion and reversible changes in cancer cell properties (15). For example, taking breast cancer as a model, it has been recently shown that the proportions of different phenotypes vary over time with a tendency to return back to equilibrium. This was found to take place stochastically, and CSCs were found to arise from non-stem-like cells (19). In the current study, the appearance of p75NTR-ve cells from p75NTR+ve cells could easily be explained by the asymmetrical division of CSC, but the emergence of p75NTR+ve progeny from p75NTR-ve cells is more difficult to explain, and the occurrence of a dedifferentiation process, similar to the one occurring in the above-mentioned breast cancer study, cannot be excluded. This process might occur in OSCC, similar to breast cancer, as a systematic event during cancer progression that drives the population toward initial equilibrium. Accordingly, the stem cell characteristics detected later in culture or after *in vivo* injection of the more differentiated p75NTR^{Low} cells might be attributed to the p75NTR^{High} cells generated from them by dedifferentiation. The differences in the stem cell characteristics between the two subpopulations might be then explained as a time-dependent phenomenon, as dedifferentiation of p75NTR^{Low} in p75NTR^{High} cells might take some time. Allowing more time for the p75NTR^{Low} subpopulation might perhaps lead, at some later time point, to the initial equilibrium of that particular OSCC population. The fact that p75NTR^{Low} cells were able to form tumors in immunodeficient mice, but with a longer lag phase might be also taken as a further corroboration for this hypothesis. In the same line point, also the findings from the immunohistochemical analysis of the xenografts showing that, while fully formed, the tumors initiated by the p75NTR^{Low} cells were not different from the tumors initiated by the p75NTR^{high} cells (in terms of p75NTR expression and the frequency of proliferating cells).

De novo generation of p75NTR^{High} cells from p75NTR^{Low} cells might also be a consequence of the presence of another subpopulation with stem cell features within the p75NTR^{Low} cells. The switching ability of multiple, coexistent subpopulations of OSCC cells with stem cell properties can, again, not be excluded. There are previous studies that showed that within OSCC, multiple CSC subpopulations with distinct phenotype coexist, each of them predominating at one time point and being responsible for tumor formation and self-renewal, but able to switch their phenotype between them in certain conditions. In this line, it was previously shown in OSCC that CSCs can switch between epithelial/proliferative and EMT phenotypes. This characteristic was found to be restricted to ALDH1+ cells (18); therefore, exploring the relationship between p75NTR+ and ALDH1+ subpopulations in OSCC might provide more insight into the extent to

which the CSC model is applicable to OSCC. Nevertheless, although allowing longer time for tumor formation, the p75NTR^{Low} cells could not initiate tumors with the same incidence as p75NTR^{High} cells, suggesting that, although transitory, there is an initial difference in the stem cell properties between these two populations sorted for their differential expression of p75NTR. This was also showed by the prominent difference in the expression levels of several relevant CSC genes using RNA extracted from the two subpopulations immediately after FACS sorting, indicating that p75NTR can be used for isolating a subpopulation of OSCC cells enriched for cells with stem cell-like properties in OSCC at a certain time point.

Supporting Information

Additional Supporting Information may be found in the online version of this article:

Figure S1 Comparison of the means of the expression levels, in a logarithmic scale, of stem cell- and EMT-related markers, and differentiation markers in p75NTR^{High} and p75NTR^{Low} 5PT cells, as yielded by qRT-PCR (A). Bar chart illustrating the change in the percentage of p75NTR +ve 5PT cells from day 1 to day 7 (B), error bars represent standard deviation.

References

1. Clarke MF, Dick JE, Dirks PB, et al. Cancer stem cells–perspectives on current status and future directions: AACR Workshop on cancer stem cells. *Cancer Res* 2006; **66**: 9339–44.
2. Bonnet D, Dick JE. Human acute myeloid leukemia is organized as a hierarchy that originates from a primitive hematopoietic cell. *Nat Med* 1997; **3**: 730–7.
3. Lapidot T, Sirard C, Vormoor J, et al. A cell initiating human acute myeloid leukaemia after transplantation into SCID mice. *Nature* 1994; **367**: 645–8.
4. Al-Hajj M, Wicha MS, Benito-Hernandez A, et al. Prospective identification of tumorigenic breast cancer cells. *Proc Natl Acad Sci USA* 2003; **100**: 3983–8.
5. O'brien CA, Pollett A, Gallinger S, et al. A human colon cancer cell capable of initiating tumour growth in immunodeficient mice. *Nature* 2007; **445**: 106–10.
6. Singh SK, Hawkins C, Clarke ID, et al. Identification of human brain tumour initiating cells. *Nature* 2004; **432**: 396–401.
7. Collins AT, Berry PA, Hyde C, et al. Prospective identification of tumorigenic prostate cancer stem cells. *Cancer Res* 2005; **65**: 10946–51.
8. Ho MM, Ng AV, Lam S, et al. Side population in human lung cancer cell lines and tumors is enriched with stem-like cancer cells. *Cancer Res* 2007; **67**: 4827–33.
9. Yang ZF, Ho DW, Ng MN, et al. Significance of CD90+ cancer stem cells in human liver cancer. *Cancer Cell* 2008; **13**: 153–66.
10. Fang D, Nguyen TK, Leishear K, et al. A tumorigenic subpopulation with stem cell properties in melanomas. *Cancer Res* 2005; **65**: 9328–37.
11. Jiang X, Zhao Y, Smith C, et al. Chronic myeloid leukemia stem cells possess multiple unique features of resistance to BCR-ABL targeted therapies. *Leukemia* 2007; **21**: 926–35.
12. Donnenberg VS, Donnenberg AD. Multiple drug resistance in cancer revisited: the cancer stem cell hypothesis. *J Clin Pharmacol* 2005; **45**: 872–7.
13. Brabletz T, Jung A, Spaderna S, et al. Opinion: migrating cancer stem cells – an integrated concept of malignant tumour progression. *Nat Rev Cancer* 2005; **5**: 744–9.
14. Chen SF, Chang YC, Nieh S, et al. Nonadhesive culture system as a model of rapid sphere formation with cancer stem cell properties. *PLoS One* 2012; **7**: e31864.
15. Meacham CE, Morrison SJ. Tumour heterogeneity and cancer cell plasticity. *Nature* 2013; **501**: 328–37.
16. Shackleton M, Quintana E, Fearon ER, et al. Heterogeneity in cancer: cancer stem cells versus clonal evolution. *Cell* 2009; **138**: 822–9.
17. Odoux C, Fohrer H, Hoppo T, et al. A stochastic model for cancer stem cell origin in metastatic colon cancer. *Cancer Res* 2008; **68**: 6932–41.
18. Biddle A, Liang X, Gammon L, et al. Cancer stem cells in squamous cell carcinoma switch between two distinct phenotypes that are preferentially migratory or proliferative. *Cancer Res* 2011; **71**: 5317–26.
19. Gupta PB, Fillmore CM, Jiang G, et al. Stochastic state transitions give rise to phenotypic equilibrium in populations of cancer cells. *Cell* 2011; **146**: 633–44.
20. Prince ME, Sivanandan R, Kaczorowski A, et al. Identification of a subpopulation of cells with cancer stem cell properties in head and neck squamous cell carcinoma. *Proc Natl Acad Sci USA* 2007; **104**: 973–8.
21. Clay MR, Tabor M, Owen JH, et al. Single-marker identification of head and neck squamous cell carcinoma cancer stem cells with aldehyde dehydrogenase. *Head Neck* 2010; **9**: 1195–201.
22. Zhang P, Zhang Y, Mao L, et al. Side population in oral squamous cell carcinoma possesses tumor stem cell phenotypes. *Cancer Lett* 2009; **277**: 227–34.
23. Nakamura T, Endo K, Kinoshita S. Identification of human oral keratinocyte stem/progenitor cells by neurotrophin receptor p75 and the role of neurotrophin/p75 signaling. *Stem Cells* 2007; **25**: 628–38.
24. Okumura T, Shimada Y, Imamura M, et al. Neurotrophin receptor p75(NTR) characterizes human esophageal keratinocyte stem cells *in vitro*. *Oncogene* 2003; **22**: 4017–26.
25. Aggarwal BB. Signalling pathways of the TNF superfamily: a double-edged sword. *Nat Rev Immunol* 2003; **3**: 745–56.
26. Roux PP, Barker PA. Neurotrophin signaling through the p75 neurotrophin receptor. *Prog Neurobiol* 2002; **67**: 203–33.
27. Li X, Shen Y, Di B, et al. Biological and clinical significance of p75NTR expression in laryngeal squamous epithelia and laryngocarcinoma. *Acta Otolaryngol* 2012; **132**: 314–24.
28. Walch ET, Marchetti D. Role of neurotrophins and neurotrophins receptors in the *in vitro* invasion and heparanase production of human prostate cancer cells. *Clin Exp Metastasis* 1999; **17**: 307–14.
29. Wilmet JP, Tastet C, Desruelles E, et al. Proteome changes induced by overexpression of the p75 neurotrophin receptor (p75NTR) in breast cancer cells. *Int J Dev Biol* 2011; **55**: 801–9.
30. Civenni G, Walter A, Kobert N, et al. Human CD271-positive melanoma stem cells associated with metastasis establish tumor heterogeneity and long-term growth. *Cancer Res* 2011; **71**: 3098–109.
31. Huang SD, Yuan Y, Liu XH, et al. Self-renewal and chemotherapy resistance of p75NTR positive cells in esophageal squamous cell carcinomas. *BMC Cancer* 2009; **9**: 9.

32. Kiyosue T, Kawano S, Matsubara R, et al. Immunohistochemical location of the p75 neurotrophin receptor (p75NTR) in oral leukoplakia and oral squamous cell carcinoma. *Int J Clin Oncol* 2011; **1**: 154–63.
33. Soland TM, Brusevold IJ, Koppang HS, et al. Nerve growth factor receptor (p75 NTR) and pattern of invasion predict poor prognosis in oral squamous cell carcinoma. *Histopathology* 2008; **53**: 62–72.
34. Dalley AJ, Abdulmajeed AA, Upton Z, et al. Organotypic culture of normal, dysplastic and squamous cell carcinoma-derived oral cell lines reveals loss of spatial regulation of CD44 and p75(NTR) in malignancy. *J Oral Pathol Med* 2012; **42**: 37–46.
35. Harper LJ, Piper K, Common J, et al. Stem cell patterns in cell lines derived from head and neck squamous cell carcinoma. *J Oral Pathol Med* 2007; **36**: 594–603.
36. Costea DE, Dimba AO, Loro LL, et al. The phenotype of *in vitro* reconstituted normal human oral epithelium is essentially determined by culture medium. *J Oral Pathol Med* 2005; **34**: 247–52.
37. Osman TA, Oijordsbakken G, Costea DE, et al. Successful triple immunoenzymatic method employing primary antibodies from same species and same immunoglobulin subclass. *Eur J Histochem* 2013; **57**: e22.
38. Sapkota D, Bruland O, Costea DE, et al. S100A14 regulates the invasive potential of oral squamous cell carcinoma derived cell-lines *in vitro* by modulating expression of matrix metalloproteinases, MMP1 and MMP9. *Eur J Cancer* 2011; **47**: 600–10.
39. Costea DE, Gammon L, Kitajima K, et al. Epithelial stem cells and malignancy. *J Anat* 2008; **213**: 45–51.
40. Harper LJ, Costea DE, Gammon L, et al. Normal and malignant epithelial cells with stem-like properties have an extended G2 cell cycle phase that is associated with apoptotic resistance. *BMC Cancer* 2010; **10**: 166.
41. Urdiales JL, Becker E, Andrieu M, et al. Cell cycle phase-specific surface expression of nerve growth factor receptors TrkA and p75(NTR). *J Neurosci* 1998; **18**: 6767–75.
42. Gemenetzidis E, Elena-Costea D, Parkinson EK, et al. Induction of human epithelial stem/progenitor expansion by FOXM1. *Cancer Res* 2010; **70**: 9515–26.
43. Okumura T, Tsunoda S, Mori Y, et al. The biological role of the low-affinity p75 neurotrophin receptor in esophageal squamous cell carcinoma. *Clin Cancer Res* 2006; **12**: 5096–103.

Acknowledgements

The authors would like to thank Marianne Enger for her technical assistant with the FACS and cell cycle analysis. We would also like to express our gratitude to prof. Ian Mackenzie and PhD Adrian Biddle for their fruitful discussions and for providing the cell lines.

Funding sources

Bergen Medical Research Foundation (D.E. Costea; Grant No. 20/2009), The Norwegian Cancer Research Association (D.E. Costea; Grant No. 515970/2011), and Helse Vest (De Costea Grant No. 911902/2013), Norwegian Government through Quota Programme (TO) and Center for International Health (ACJ).

Conflict of interests

None to declare.